

AD-A129 916

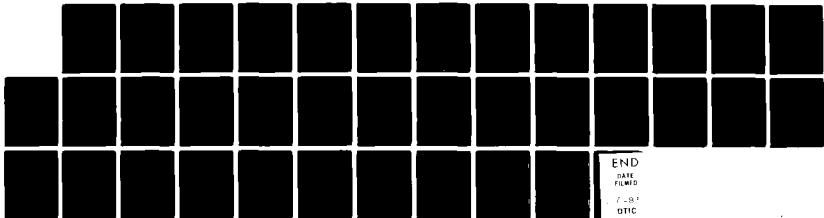
LECTURES ON MATHEMATICAL COMBUSTION LECTURE 10
FREE-BOUNDARY PROBLEMS..(U) CORNELL UNIV ITHACA NY DEPT
OF THEORETICAL AND APPLIED MECHAN..
J D BUCKMASTER ET AL. JAN 83 TR-155

1/1

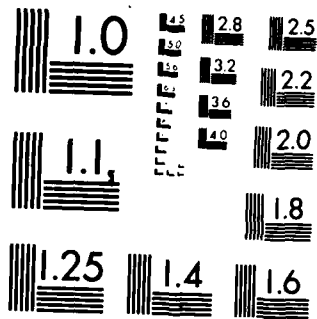
UNCLASSIFIED

F/G 21/2

ML



END
HARE
FILMED
FBI
DTIC



MICROCOPY RESOLUTION TEST CHART
NATIONAL BUREAU OF STANDARDS 1963-A

ARO 18243.26-MA

12

Cornell University



LECTURES ON MATHEMATICAL COMBUSTION

Lecture 10: Free-Boundary Problems

Technical Report No. 155

J.D. Buckmaster & G.S.S. Ludford

January 1983

ADA 1 299 16

Theoretical and Applied Mechanics

DTIC

JUN 30 1983

A

**Thurston Hall
Ithaca, New York**

DTIC FILE COPY

83 06 30 010

LECTURES ON MATHEMATICAL COMBUSTION

Lecture 10: Free-Boundary Problems

Technical Report No. 155

J.D. Buckmaster & G.S.S. Ludford

January 1983

U.S. Army Research Office
Research Triangle Park, NC 27709

Contract No. DAAG29-81-K-0127

Cornell University
Ithaca, NY 14853

Approved for public release; distribution unlimited.

The view, opinions, and/or findings contained in this report are those of the authors and should not be construed as an official Department of the Army position, policy or decision, unless so designated by other authorized documents.

Contents

	Page
1. The Hydrodynamic Limit	1
2. The Burke-Schumann Limit	3
3. NEF Tips	5
4. NEF Wall-Quenching	8
5. Straining NEFs	13
6. Shearing NEFs	15
Appendix. The Method of Lines	16
References	19
Captions	20
Figures 1-9	21

Accession For

1951 FBI

1951 FBI

1951 FBI

1951 FBI

1951 FBI

1951 FBI

1951 FBI

1951 FBI

1951 FBI

1951 FBI

1951 FBI

1951 FBI

1951 FBI

1951 FBI

1951 FBI

1951 FBI

1951 FBI

1951 FBI

1951 FBI

1951 FBI

1951 FBI

1951 FBI

1951 FBI

1951 FBI

1951 FBI

Lecture 10

FREE-BOUNDARY PROBLEMS

Throughout these lectures we have ensured that the reaction terms vanish everywhere except in a thin (flame) sheet, whose location has to be found as part of the solution. So far this free boundary has been either a plane, a circular cylinder, a sphere, or a perturbation of one of these; we now consider problems with more complicated free boundaries.

There are four different ways of confining the reaction to a sheet.

- (i) Adopt the δ -function model discussed in lecture 7.
- (ii) Take the hydrodynamic limit.
- (iii) Take the Burke-Schumann limit.
- (iv) Use activation-energy asymptotics.

In this lecture, which is an expanded version of Buckmaster (1982), we shall briefly mention examples of (ii) and (iii), but most of the discussion will deal with parabolic problems for premixed flames that arise from (iv).

1. The Hydrodynamic Limit

The jump conditions (3.9),^(3.10) imply that the flow will be diffracted by an inclined flame **Surface**. If the flame speed W is much smaller than the speed U of the fresh gas, i.e.

$$W = \epsilon U \quad \text{with} \quad \epsilon \ll 1, \quad (1)$$

a uniform flow

$$\mathbf{v}^i = (U, 0) \quad (2)$$

is turned by a plane flame so that the velocity of the burnt gas is

$$\mathbf{v}^e = (U, \pm \epsilon U(\sigma - 1)) + o(\epsilon, \epsilon), \quad (3)$$

where the sign is opposite to that of the flame slope (figure 1). The corresponding jump in pressure across the flame is $O(\epsilon)$. Such a deflection of the streamlines is a fundamental characteristics of tube flames (figure 2), which are often slender (i.e. correspond to small ϵ).

In order to describe the shape of the flame when the prescribed efflux from the tube is the plane flow $U(f(\eta), 0)$, we look for i(nterior) and e(xterior) solutions

$$u = \begin{cases} Uf(\eta) + \epsilon u_1^i(\epsilon\chi, \eta) + \dots \\ Uf(\eta) + \epsilon u_1^e(\epsilon\chi, \eta) + \dots \end{cases}, \quad v = \begin{cases} \epsilon^2 v_2^i(\epsilon\chi, \eta) + \dots \\ \epsilon v_1^e(\epsilon\chi, \eta) + \dots \end{cases} \quad (4)$$

These expansions are consistent with the slender-flame approximation, Euler's equations, and the jump conditions. Both the flame shape and the flow field can be constructed in a straightforward manner (Buckmaster & Crowley 1982).

In fact, a differential equation for the shape

$$\eta = \pm F(\epsilon\chi) \quad (5)$$

of the flame can be deduced immediately. Since v^i is $O(\epsilon^2)$, it does not contribute to the $O(\epsilon)$ normal velocity ahead of the flame, so that the flame speed has the required value (1) if

$$1 + f(F)F' = 0, \quad (6)$$

a result that is also true for axisymmetric flow. When

$$f(\eta) = 1 - \eta^2/a^2 \quad \text{with} \quad |\eta| \leq a, \quad (7)$$

i.e. the flow is Poiseuille, the flame shape is given by

$$F - F^3/3a^2 = -\epsilon\chi. \quad (8)$$

Only for slender flames can the shape be determined directly from the given flow leaving the burner.

2. The Burke-Schumann Limit

This limit arises in the context of diffusion flames as $D \rightarrow \infty$. As we saw in section 8. , the fuel is then absent on one side of the flame sheet and the oxidant on the other. The problem considered by Burke and Schumann in their seminal work was the divided flow of fuel and oxidant through concentric tubes with the flame attached to the rim of the inner tube (figure 3). If the oxidant is in excess, the flame terminates at the axis, and is said to be overventilated; if there is an excess of fuel, termination occurs at the outer tube, an underventilated condition.

Burke and Schumann neglected the effect of the flame on the flow, i.e. they adopted the constant-density approximation over 50 years ago. It is curious, in view of the enormous insight provided by their well-known analysis, that to this day one finds, at scientific forums, objections to the approximation when it is used in activation-energy asymptotics. They also neglected longitudinal diffusion, a step that can be legitimized by setting

$$\chi = x/U \tag{9}$$

and letting $U \rightarrow \infty$. The equations to be considered are then

$$\partial T / \partial \chi = \partial^2 T / \partial y^2, \quad \partial X / \partial \chi = K^{-1} \partial^2 X / \partial y^2, \quad \partial Y / \partial \chi = L^{-1} \partial^2 Y / \partial y^2 \tag{10}$$

under the jump conditions

$$\delta(T) = \delta(X) = \delta(Y) = \delta(\partial T / \partial y + 2K^{-1} \partial X / \partial y) = \delta(\partial T / \partial y + 2L^{-1} \partial Y / \partial y) = 0. \tag{11}$$

The plane version of the equations used by Burke and Schumann has been written because we shall consider a simpler, but related, problem than

theirs. General Lewis numbers have also been introduced, which necessitates a slight modification of the jump conditions derived in section 8.

Consider a plate, coincident with the negative x-axis, separating parallel and equally fast flows of oxidant and fuel (figure 4). The initial conditions are

$$T = \begin{cases} T_{f+} \\ T_{f-} \end{cases}, \quad X = \begin{cases} X_f \\ 0 \end{cases}, \quad Y = \begin{cases} 0 \\ Y_f \end{cases} \quad \text{for } y \gtrless 0 \text{ at } x = 0; \quad (12)$$

in fact, X is required to vanish everywhere below the flame sheet and Y everywhere above. The solution of the problem (10-11) can be written in terms of the similarity variable

$$\tilde{\omega} = y/x^{1/2} \quad (13)$$

as

$$X = \begin{cases} X_f \left[1 - \frac{\text{erfc}(K^{1/2}\tilde{\omega}/2)}{\text{erfc}(K^{1/2}\tilde{\omega}_*/2)} \right] \\ 0 \end{cases}, \quad Y = \begin{cases} 0 \\ Y_f \left[1 - \frac{\text{erfc}(L^{1/2}\tilde{\omega}/2)}{\text{erfc}(L^{1/2}\tilde{\omega}_*/2)} \right] \end{cases} \quad \text{for } \tilde{\omega} \gtrless \tilde{\omega}_*, \quad (14)$$

where $\tilde{\omega}_*$ is given by

$$X_f L^{1/2} e^{-K\tilde{\omega}_*^2/4} \text{erfc}(L^{1/2}\tilde{\omega}_*/2) = Y_f K^{1/2} e^{-L\tilde{\omega}_*^2/4} \text{erfc}(K^{1/2}\tilde{\omega}_*/2). \quad (15)$$

Corresponding formulas for T could also be written.

When the reactants are supplied in stoichiometric proportions (i.e. $X_f = Y_f$) and in addition $K = L$, the flame sheet coincides with the positive x-axis, i.e. $\tilde{\omega}_* = 0$. A decrease (increase) in X_f or an increase (decrease) in K moves the flame sheet up (down).

Our simple problem has yielded to analytical treatment, but in general the Burke-Schumann limit involves numerical integration of a type that arises in the free-boundary problems of activation-energy asymptotics to be treated next.

3. NEF Tips

The most interesting examples of free-boundary problems uncovered by activation-energy asymptotics concern NEF's, and discussion of these examples have almost invariably adopted the constant-density approximation. The relevant equations and jump conditions have been developed in section 4.

The starting point is a steady plane deflagration in a uniform flow with speed U greater than 1 (figure 5). The solution is

$$T = \begin{cases} T_f + Y_f e^n \\ H_f \equiv T_b \end{cases}, \quad h = \begin{cases} -\lambda Y_f n e^n \\ 0 \end{cases} \quad \text{for } n \lesssim 0, \quad (16)$$

formulas that have already been used in connection with plane-flame stability (section 5). Now consider the effect of introducing an adiabatic, non-catalytic wall at the plane $y = 0$. For simplicity we shall take $\lambda = 0$, so that h vanishes identically and the problem reduces to one for T alone, namely the free-boundary problem

$$U \partial T / \partial x = \nabla^2 T \quad \text{for } n < 0 \quad \text{and } y > 0, \quad (17)$$

$$T \rightarrow T_b, \quad \partial T / \partial n \rightarrow Y_f \quad \text{as } n \rightarrow 0-, \quad (18)$$

$$\partial T / \partial y = 0 \quad \text{at } y = 0, \quad (19)$$

$$T \rightarrow T_f + Y_f e^n \quad \text{as } x \rightarrow -\infty \quad \text{with } n \text{ fixed.} \quad (20)$$

The last condition comes from the requirement that, far from the wall, the temperature field has the description (16a); this structure gives way to a

two-dimensional combustion field as the wall is approached. Here we have the problem of a plane-flame tip for $L = 1$, the wall corresponding to the line of symmetry. No attempt has been made to solve it in this form because of its elliptic nature.

If U is large, the formulation becomes parabolic, giving a classical problem of Stefan type. Thus, introducing the coordinate (9) and letting $U \rightarrow \infty$ converts the problem (17-20) into

$$\partial T / \partial \chi = \partial^2 T / \partial y^2 \quad \text{for } 0 < y < F(\chi), \quad (21)$$

$$T \rightarrow T_b, \quad \partial T / \partial y \rightarrow Y_f \quad \text{as } y \rightarrow F(\chi)-0, \quad (22)$$

$$\partial T / \partial y = 0 \quad \text{at } y = 0, \quad (23)$$

$$T \rightarrow T_f + Y_f e^{y+\chi} \quad \text{as } \chi \rightarrow -\infty, \quad (24)$$

where

$$y = F(\chi) \quad (25)$$

is the free boundary and the origin has been taken at the intersection of the undisturbed flame with the wall, i.e.

$$\lim_{\chi \rightarrow -\infty} [F(\chi) + \chi] = 0. \quad (26)$$

This problem is identical to that of a plane flame approaching a parallel adiabatic wall, with χ playing the role of time.

The solution of the Stefan problem (21-24), and similar ones that are discussed later, must be obtained numerically. Meyer's (1977) method of lines is particularly well suited to this task and is outlined in an appendix. It was used to obtain figure 6, which reveals a significant increase in flame speed as the flame sheet approaches the axis, i.e. near

the tip. This adjustment on the diffusion-length scale of a NEF smooths out the sharp tip predicted by the hydrodynamic analysis in section 1.

A similarity solution can be constructed for such problems in the neighborhood of the tip. Setting

$$T = T_b + (\chi_t - \chi)^{1/2} G(\tilde{\omega}) \text{ with } \tilde{\omega} = (\chi_t - \chi)^{-1/2} y, \quad (27)$$

where χ_t defines the location of the tip, leads to the differential equation

$$G'' - \frac{1}{2}\tilde{\omega}G' + \frac{1}{2}G = 0 \quad (28)$$

and the boundary conditions

$$G'(0) = 0, G(\omega_*) = 0, G'(\omega_*) = Y_f. \quad (29)$$

Here the constant $\tilde{\omega}_*$, which has to be found, determines the locally parabolic flame sheet. The solution of equation (28) satisfying the conditions (29b,c) is

$$G = Y_f \tilde{\omega}_* e^{-\tilde{\omega}_*^2/4} \tilde{\omega} \int_{\tilde{\omega}_*}^{\tilde{\omega}} e^{x^2/4} dx/x^2; \quad (30)$$

the condition (29a) is then satisfied if

$$\tilde{\omega}_* e^{-\tilde{\omega}_*^2/4} \int_0^{\tilde{\omega}_*/2} e^{x^2} dx = 1, \text{ i.e. } \omega_* = 1.85. \quad (31)$$

The similarity solution breaks down in the neighborhood of the tip where the flame slope is $O(1)$, but the extent of this neighborhood is given by

$$\chi_t - \chi = O(U^{-2}) \quad (32)$$

and, hence, can be made arbitrarily small by taking U large enough.

For $z \neq 0$, i.e. $L \neq 1$, the function h no longer vanishes and the problem (21-24) must be augmented with equations and conditions for h , in particular

$$\partial h / \partial y = 0 \quad \text{for } y = 0. \quad (33)$$

The effects of Lewis number are also shown in figure 6. Decreasing from 1 causes the tip to elongate and eventually assume a bulbous form. It is tempting to terminate solutions of the latter type at the point Q in figure 6, for they then closely resemble the open flame tips seen in the combustion of lean hydrogen or rich heavy-hydrocarbon mixtures, mixtures for which the effective Lewis number is significantly less than 1. But the mathematics gives no clear-cut reason for doing this; the only suggestion is the marked decrease in temperature along the flared portion of the flame.

The negative flame speeds associated with those portions of the flame with positive slope, although curious, do not violate the physics. There is a diffusive flux of reactant in the y -direction towards the flame sheet to maintain the combustion.

4. NEP Wall-Quenching

When the wall is not adiabatic, the problem is no longer relevant to flame tips. For a cooled wall it models, in a rough sense, the behavior of a flame near a burner rim (figure 7). It corresponds more precisely to the propagation of a plane wave towards a parallel cooled wall, but our discussion will be couched in terms of burner flames.

A flame can be stabilized on a Bunsen burner only under a limited range of conditions. Outside this range either "blow-off" will occur so that the flame becomes detached from the burner, or "flashback" will take place, the flame traveling to the base of the burner via

the inner wall of the tube. The tendency for flashback is easy to understand: a premixed flame will travel upstream unless the gas speed is greater than the flame speed, and at the surface of the burner tube the gas speed falls to zero. Flashback is, therefore, inevitable unless there is some mechanism to prevent the flame from reaching the surface. Heat transfer from the gas to the tube, quenching the reaction that sustains the flame, is commonly regarded as one such mechanism; the free-boundary problem under discussion illustrates this mechanism.

The boundary conditions at the wall are taken to be

$$\partial T / \partial y = k(T - T_f) / \theta, \quad \partial Y / \partial y = 0 \quad \text{at} \quad y = 0, \quad (34)$$

i.e.

$$\partial T / \partial y = 0, \quad \partial h / \partial y = k(T - T_f) \quad \text{at} \quad y = 0 \quad (35)$$

in the NEF formulation. At the same time, the problem will be generalized slightly by considering a not necessarily uniform flow

$$v = (Uf(y), 0) \quad \text{as} \quad U \rightarrow \infty. \quad (36)$$

This is more realistic than a uniform flow when the no-slip condition at the wall is satisfied by taking $f(0) = 0$. We shall set $\ell = 0$ so as to filter out the enthalpy loss or gain at the flame due to unbalanced diffusion of temperature and reactant.

The problem is again numerical, but certain features can be derived analytically. So long as the flame intersects the wall, a similarity solution describes its behavior there; when it extends to $\chi = \infty$, there is an asymptotic solution.

Consider first

$$f(y) \equiv 1; \quad (37)$$

later we will briefly discuss the more realistic choice (55). We shall assume that

$$T \rightarrow T_0 \text{ as } \chi \rightarrow \infty, \quad (38)$$

the approach being exponential in χ , and that

$$\chi^{-\frac{1}{2}} F(\chi) \rightarrow 0 \text{ as } \chi \rightarrow \infty, \quad (39)$$

where F is the free-boundary function (25). Self-consistency of the resulting asymptotic description will be checked in due course.

We start with the problem for h (which has no jumps at the flame sheet) and write

$$h = h^{(1)} + h^{(2)} + h^{(3)}, \quad (40)$$

where $h^{(1)}, h^{(2)}, h^{(3)}$ satisfy the heat equation (21) individually, the boundary conditions

$$\partial h^{(1)}/\partial y = kY_f, \quad \partial h^{(2)}/\partial y = 0, \quad \partial h^{(3)}/\partial y = k(T - T_f - Y_f) \text{ at } y=0, \quad (41)$$

and vanish exponentially rapidly as $y \rightarrow \infty$. The condition (38) ensures that $h^{(3)}$ is exponentially small as $\chi \rightarrow \infty$ and so need not be considered further. The asymptotic behaviors of the two remaining functions are determined by similarity solutions of the heat equation. Thus

$$h^{(1)} = \chi^{\frac{1}{2}} G(\tilde{\omega}) \text{ with } \tilde{\omega} = y/\chi^{\frac{1}{2}}, \quad G = kY_f [\tilde{\omega} \operatorname{erfc}(\tilde{\omega}/2) - (2/\sqrt{\pi}) e^{-\tilde{\omega}^2/4}] \quad (42)$$

and $h^{(2)}$ is asymptotically a sum of the eigensolutions

$$\chi^{-\frac{1}{2}-r} E(\tilde{\omega}) \text{ with } E = e^{-\tilde{\omega}^2/8} D_{2n}(\tilde{\omega}/\sqrt{2}); \quad (43)$$

here n is a non-negative integer and D is the parabolic cylinder function. Since all the eigensolutions vanish as $\chi \rightarrow \infty$, we need not consider $h^{(2)}$ further.

Only $h^{(1)}$ is left and from it we find

$$h/\chi^{\frac{1}{2}} = -2kY_f/\sqrt{\pi} + O(\tilde{\omega}) \text{ for } \tilde{\omega} \text{ small.} \quad (44)$$

In view of the hypothesis (39), setting $\tilde{\omega} = \chi^{-\frac{1}{2}}F$ in this expansion gives the value of h at the flame sheet, so that

$$\phi_* = (2kY_f/\sqrt{\pi T_b^2})\chi^{\frac{1}{2}}[1+o(1)] \text{ as } \chi \rightarrow \infty. \quad (45)$$

Consider now the asymptotic behavior of

$$T = T_b + Y_f \bar{T}. \quad (46)$$

The appropriate modification of the problem (21-24) is

$$\partial \bar{T} / \partial \chi = \partial^2 \bar{T} / \partial y^2 \text{ for } 0 < y < F(\chi), \quad (47)$$

$$\bar{T} \rightarrow 0, \quad \partial \bar{T} / \partial y \rightarrow \exp(-\phi_*/2) \text{ as } y \rightarrow F(\chi) - 0, \quad (48)$$

$$\partial \bar{T} / \partial y = 0 \text{ at } y = 0; \quad (49)$$

the initial conditions (at $\chi = -\infty$) are omitted. The solution is

$$F(\chi) \sim \tilde{\omega}_* \chi^{\frac{1}{2}}, \quad \bar{T} \sim \exp(-kY_f \chi^{\frac{1}{2}} / \sqrt{\pi T_b^2}) \chi^{\frac{1}{2}} G(\tilde{\omega}) \text{ with } \tilde{\omega} = y/\chi^{\frac{1}{2}}, \quad (50)$$

where

$$G'' + a^2 G = 0, \quad G'(0) = 0, \quad G(\tilde{\omega}_*) = 0, \quad G'(\tilde{\omega}_*) = 1 \text{ with } a^2 = kY_f / 2\sqrt{\pi T_b^2}. \quad (51)$$

Note that the result (50a) is consistent with the assumption (39) under which it was obtained. The constant $\tilde{\omega}_*$, which has to be bound, determines the asymptotic shape (50a) of the flame sheet. The solution of the equation (51a) satisfying the conditions (51b,d) is

$$G = -\cos a\tilde{\omega} / a \sin a\tilde{\omega}_*; \quad (52)$$

the condition (51c) is then satisfied if

$$a\bar{\omega}_* = (n + \frac{1}{2})\pi \quad (53)$$

for some integer n. A further requirement comes from the maximum principle for the heat equation, namely $T \leq T_b$ everywhere. The only acceptable n is zero and we have

$$\bar{\omega}_* = \pi^{5/4} T_b / \sqrt{2kY_f} \quad (54)$$

A similar analysis is possible when

$$f(y) \equiv y, \quad (55)$$

a more realistic choice physically. Now

$$h^{(1)} = \chi^{-1/3} G(\bar{\omega}) \text{ with } \bar{\omega} = y/\chi^{1/3}, G = kY_f \bar{\omega} \Gamma(-1/3, \bar{\omega}^3/9) / \Gamma(-1/3), \quad (56)$$

so that

$$h/\chi^{1/3} = -3^{2/3} kY_f / \Gamma(2/3) + o(\bar{\omega}) \text{ for } \bar{\omega} \text{ small}; \quad (57)$$

and

$$\phi_* = (3^{2/3} kY_f / \Gamma(2/3) T_b^2) \chi^{1/3} [1 + o(1)] \text{ as } \chi \rightarrow \infty \quad (58)$$

provided

$$\chi^{-1/3} F(\chi) \rightarrow 0 \text{ as } \chi \rightarrow \infty. \quad (59)$$

The \bar{T} -problem has the solution

$$\bar{T}(\chi) = \bar{\omega}_* \chi^{2/9}, \bar{T} = \exp(-3^{2/3} kY_f \chi^{1/3} / 2\Gamma(2/3) T_b^2) \chi^{2/9} G(\bar{\omega}) \text{ with } \bar{\omega} = y/\chi^{2/9}, \quad (60)$$

where

$$G'' + a^2 \chi G = 0, G'(0) = 0, G(\bar{\omega}_*) = 0, G'(\bar{\omega}_*) = 1 \text{ with } a^3 = 3^{-1/3} kY_f / 2\Gamma(2/3) T_b^2. \quad (61)$$

Finally, the maximum principle leads us, as before, to the conclusion that

$$G = -\frac{\bar{\omega}^{1/2} J_{-1/3}(2a\bar{\omega}^{3/2}/3)}{a\bar{\omega}_* J_{2/3}(2a\bar{\omega}_*^{3/2}/3)}, \quad \omega_* = \left(\frac{3^{7/3} \Gamma(2/3) T_b^2 r^2}{2kY_r} \right)^{1/3}, \quad (62)$$

where r is the smallest zero of $J_{-1/3}(r)$.

These results suggest a simple dichotomy: for sufficiently small heat loss, the flame eventually intersects the wall (a necessary condition for flashback); but for larger values of k the flame ultimately moves away from the wall, in particular according to the result (60a) for the flow (55), and flashback cannot occur. Figure 8 shows Buckmaster's numerical solutions; clearly an increase in k tends to reduce the flame speed near the wall. For moderate values of k , he obtained slightly bulbous shapes (cf. flame tips for $L < 1$), suggesting that this would be the case for all sufficiently large k . Numerical re-examination of question has, however, provided good evidence that the dichotomy mentioned above does indeed occur.

5. Straining NEFs

So far we have dealt only with parallel flows, but parabolic free-boundary problems can also be formulated for the more general velocity fields

$$\bar{y} = Uq(x/U, y/U) \text{ with } U \gg 1. \quad (63)$$

These are fast flows with $\nabla \bar{y} = O(1)$; more precisely, each is effectively made up of an uniform flow and a simple strain, both of which vary slowly. The angle between the flame and the streamlines is small, so that it stays close to a single streamline. If χ is measured along the streamline and y perpendicular to it, the velocity in the neighborhood of the streamline is approximated by

$$\bar{y} = (Uq_0, -q_0'y) \quad (64)$$

where $q_0(\chi)$ is the speed on $y = 0$. In the limit $U \rightarrow \infty$ the NEF equations (4.) become

$$(q_0 \partial/\partial x - q_0' y \partial/\partial y)(T, h) = \partial^2(T, h + \epsilon T)/\partial y^2, \quad (65)$$

and these are amenable to numerical treatment for any choice of q_0 . Modest variations in ϵ do not have a substantial qualitative effect, so that we shall set $\epsilon = 0$.

Two examples will be considered, namely

$$q_0(\chi) = .35 \sin \chi \quad \text{for } 0 < \chi < \pi, \quad .35(\chi - 2\chi^3/3 - \chi^5/5) \quad \text{for } \chi > 0. \quad (66)$$

Each of these has a stagnation point as $\chi \rightarrow 0$, where the analysis leading to equations (65) breaks down; nevertheless the corresponding stagnation-point solution constructed in section 4. provides the correct initial conditions. Figure 9 shows, for each example, a correlation between the flame speed W and the strain rate q_0' , a measure of the stretch experienced by an element of the flame: as the stretch increases (decreases) the flame speed decreases (increases).

The conclusion is not necessarily valid in other circumstances, however, as can be seen from analytical results obtained by Buckmaster (1932) for a general, small but rapid velocity change

$$q_0 = 1 + \epsilon Q(\bar{\chi}) \quad \text{with } 0 < \epsilon \ll 1, \quad \bar{\chi} = \chi/\epsilon^2 \quad (67)$$

on the scale of χ . The wave speed has the explicit representation

$$W(\bar{\chi}) = 1 - \frac{1}{\sqrt{\pi}} \int_{-\infty}^{\bar{\chi}} \frac{Q'(\mu)}{\sqrt{\bar{\chi} - \mu}} d\mu, \quad (68)$$

a formula that, surprisingly enough, is valid for all values of ϵ . There is no strong connection between the behavior of W and changes in the stretch

$\epsilon Q'$; in fact, a change in the sign of the stretch has more influence on W .

The result (68) shows that Q can be chosen (with a degree of arbitrariness) to make W vanish at any given point. The possibility of decreasing the flame speed to zero at a point by adjusting the velocity field has not been demonstrated before.

6. Shearing NEFs

We conclude our discussion of free-boundary problems by briefly describing the effect of shear on a premixed flame. The wall is removed and a linear shear flow is inserted for $y < 0$, the flow being assumed uniform for $y > 0$. More precisely,

$$f(y) = \begin{cases} 1 \\ 1-\omega y \end{cases} \quad \text{for } y \gtrless 0 \quad (69)$$

in the expression (36).

Numerical results have been obtained, in particular for $\omega = 5$. Here we shall be content to describe the solution in the limit of very strong shear, i.e. $\omega \rightarrow \infty$. Then the equations in the lower half-plane simplify to

$$\partial T / \partial \chi = \partial h / \partial \chi = 0, \quad (70)$$

giving the solution

$$T = T_f, \quad h = 0; \quad (71)$$

these become boundary conditions (at $y = 0$) on the solution in the upper half-plane.

The asymptotic behavior as $\chi \rightarrow \infty$ is particularly simple, depending only on y :

$$T = \begin{cases} T_f + Y_f Y / F(\infty) \\ T_b \end{cases}, \quad h = \begin{cases} -2Y_f Y / F(\infty) \\ -2Y_f \end{cases} \quad \text{for } y \lesseqgtr F(\infty), \quad (72)$$

where

$$F(\infty) = e^{\frac{1}{2}}. \quad (73)$$

Numerical integration shows how the remote combustion field (16) is transformed into the asymptotic field (72). The flame speed vanishes as $\chi \rightarrow \infty$ and is negative or positive in the neighborhood of infinity accordingly as λ is positive or negative.

Appendix. The Method of Lines

Consider the parabolic free-boundary problem (21-24). Let

$$T_n(y) = T(\chi_n, y), \quad F_n = F(\chi_n), \quad (74)$$

and approximate the partial differential equation (21) by the ordinary differential equation

$$T_n'' = T_n / \Delta\chi - T_{n-1} / \Delta\chi \quad \text{with } \Delta\chi = \chi_n - \chi_{n-1}. \quad (75)$$

Having determined T_{n-1} at the previous step, we must integrate this second-order equation for T_n along the line $\chi = \chi_n$ subject to three boundary conditions (22,23). The integration will, therefore, determine not only T_n but also F_n .

Let $A(y)$ be the solution of equation (75) with $A(0) = 1, A'(0) = 0$ and let $B(y)$ be the solution with $A(0) = A'(0) = 1$. Then

$$T_n = (A-B)b + B \quad (76)$$

is the solution satisfying

$$T_n(0) = b, \quad T_n'(0) = 0, \quad (77)$$

and from it we may calculate

$$T'_n = (A'-B')b + B'. \quad (78)$$

Elimination of b from the equations (75),(78) gives a relation of the form

$$T'_n = PT_n + Q, \quad (79)$$

where $P(y)$ and $Q(y)$ could be written in terms of A and B . The initial conditions (77) show that

$$P(0) = Q(0) = 0, \quad (80)$$

since P, Q (like A, B) are independent of the parameter b . The key step is to find differential equations for P, Q .


If T'_n and T''_n are eliminated between the two equations (75), (79) we are left with

$$T_n(P' + P^2 - 1/\Delta\chi) + (Q' + PQ + T_{n-1}/\Delta\chi) = 0. \quad (81)$$

Since only T_n depends on b , the parentheses must separately vanish, giving a pair of first-order differential equations for P, Q . Numerical integration, under the initial conditions (80), then determines these functions.

The position $y = F_n$ of the free boundary can now be determined as a root of the equation

$$Y_f = P(F_n)T_b + Q(F_n), \quad (82)$$

obtained by substituting the flame-sheet conditions (22) in the relation (79). With F found in this way, the relation 

(considered as a first-order differential equation for T_n) can be integrated towards $y = 0$ with the initial condition $T_n(F_n) = T_b$, to determine $T_n(y)$.

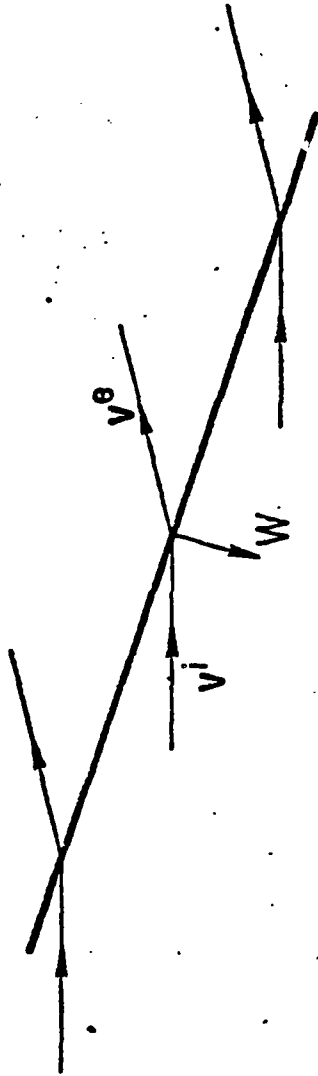
The method is quick, efficient, and requires no iterations.

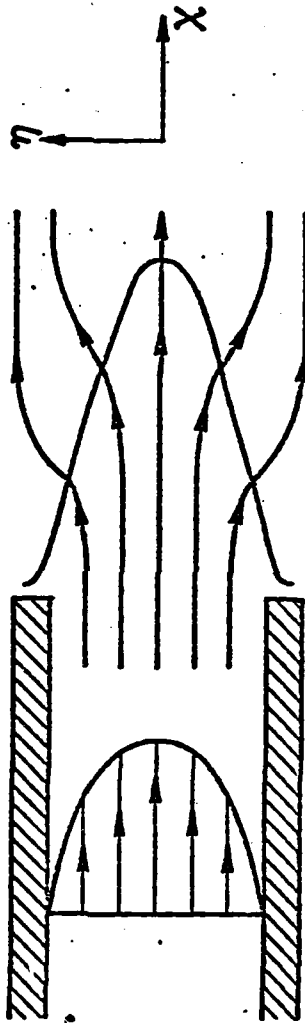
References

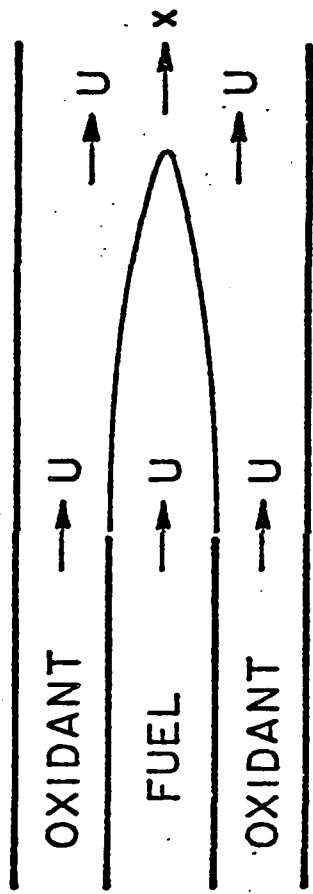
1. Buckmaster, J.D. (1982). Two examples of a stretched flame. Quarterly Journal of Mechanics and Applied Mathematics 35, 249-263.
2. Buckmaster, J.D. (1983). Free boundary problems in combustion. Proceedings of the 1981 Montecatini Symposium on Free Boundary Problems, Springer-Verlag.
3. Buckmaster, J.D. & Crowley, A. The fluid mechanics of flame tips. (Submitted for publication.)
4. Meyer, G. (1977). One-dimensional parabolic free boundary problems. SIAM Review 19, 17-34.

Captions

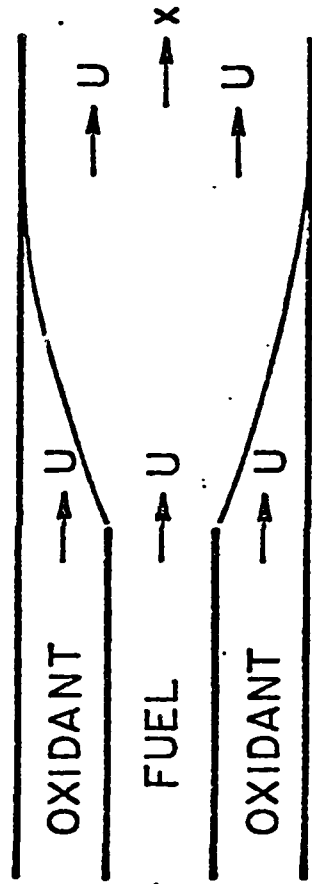
- 10.1 Diffraction of streamlines at flame surface.
- 10.2 Tube flame.
- 10.3 Burke-Schumann's problem: diffusion flame (a) over-ventilated, (b) underventilated.
- 10.4 Simpler version of Burke-Schumann problem.
- 10.5 Plane flame in uniform flow.
- 10.6 Plane NEF tips.
- 10.7 Flame near a burner rim.
- 10.8 Flame-sheet profiles for cold-wall problem.
- 10.9 Variation of flame speed W and stretch q'_0 with χ for the more general non-uniform velocity fields (66a,b).



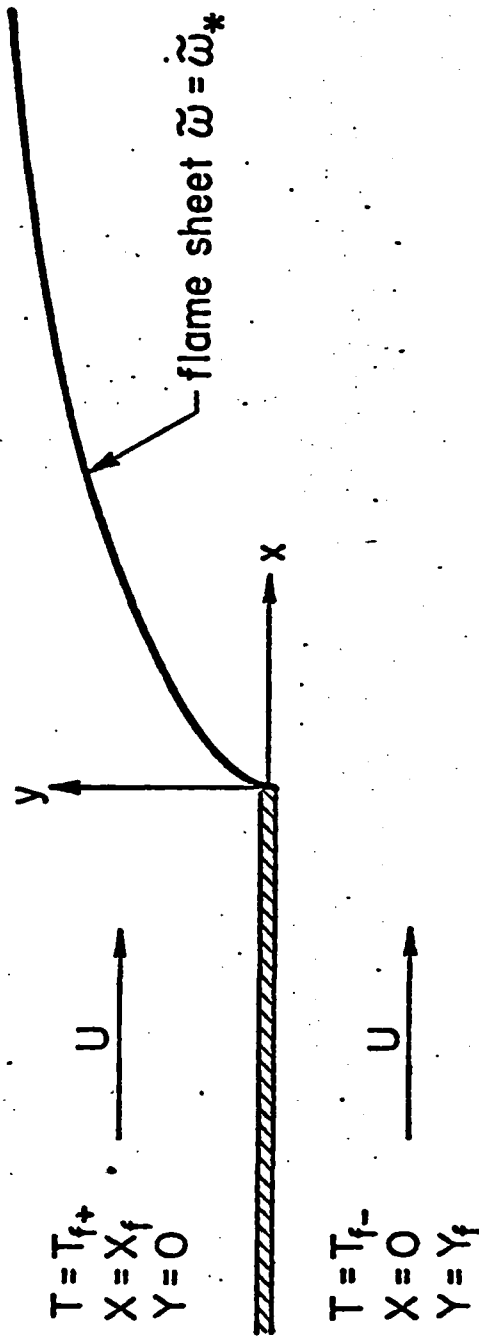


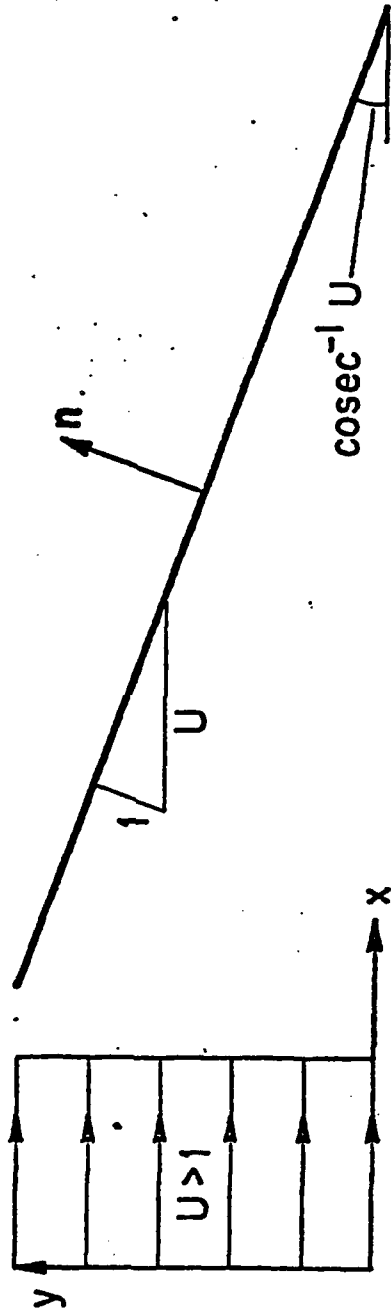


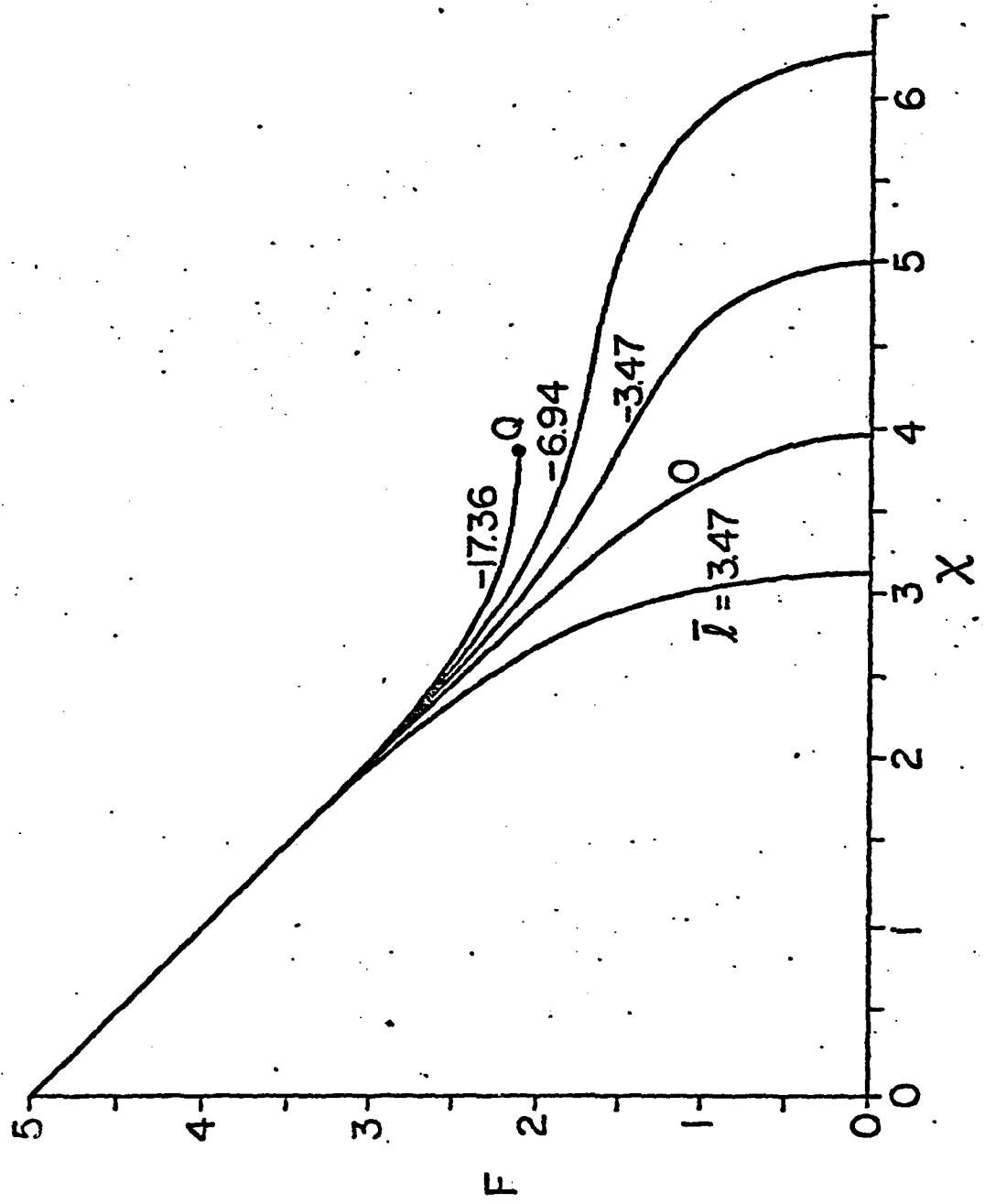
(a)

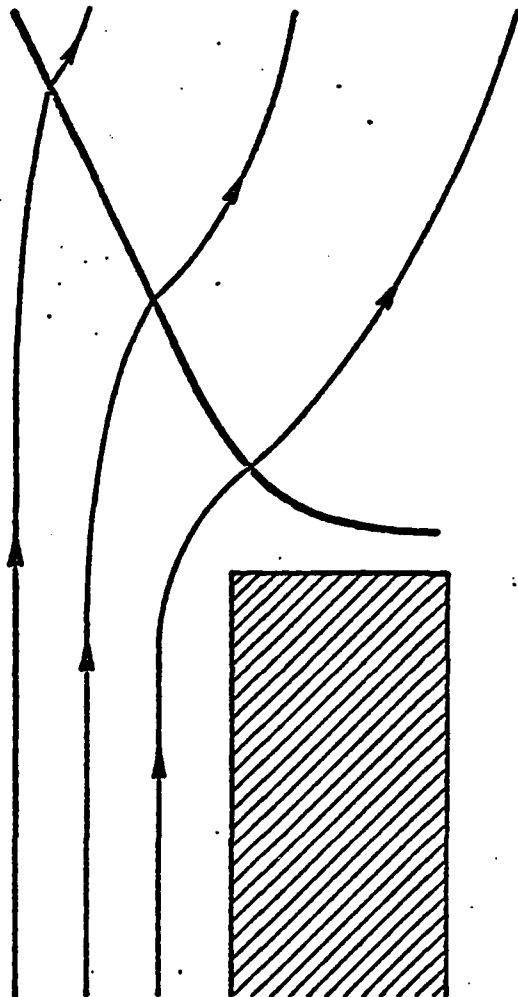


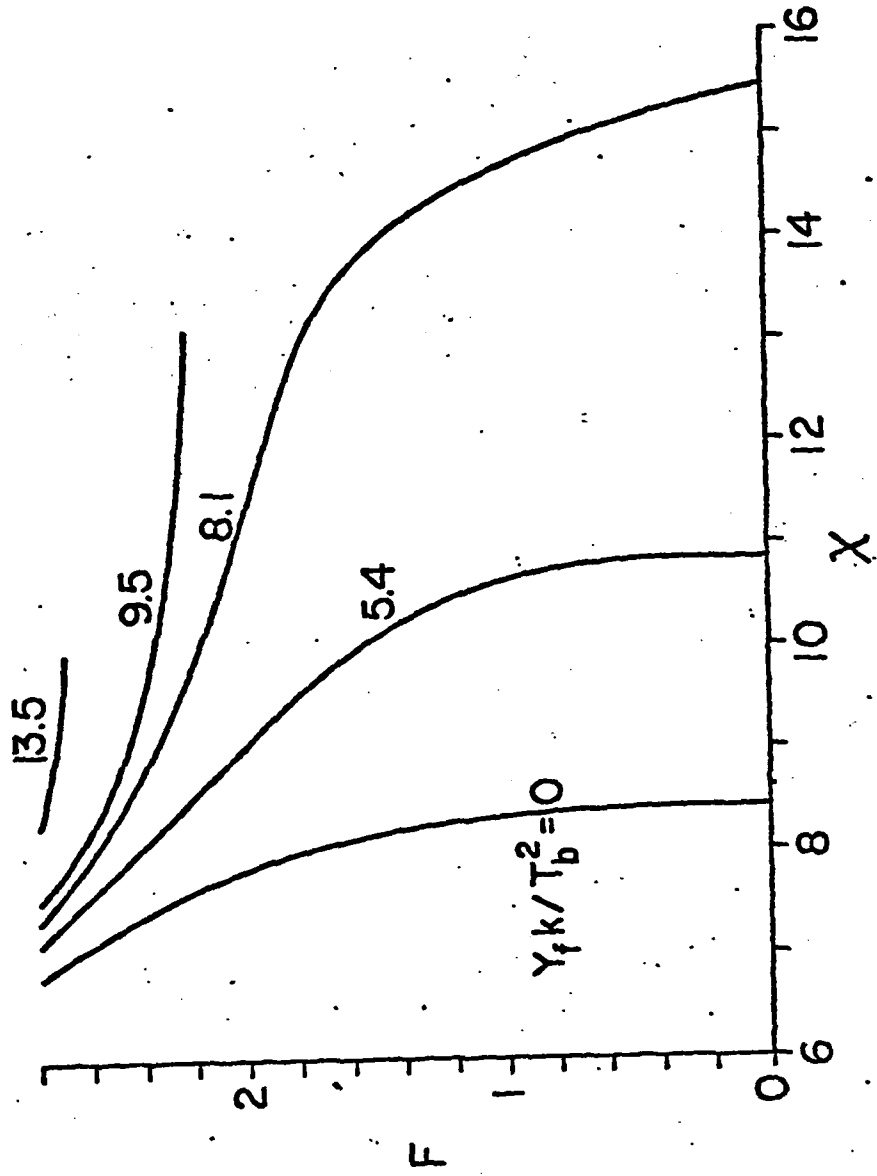
(b)

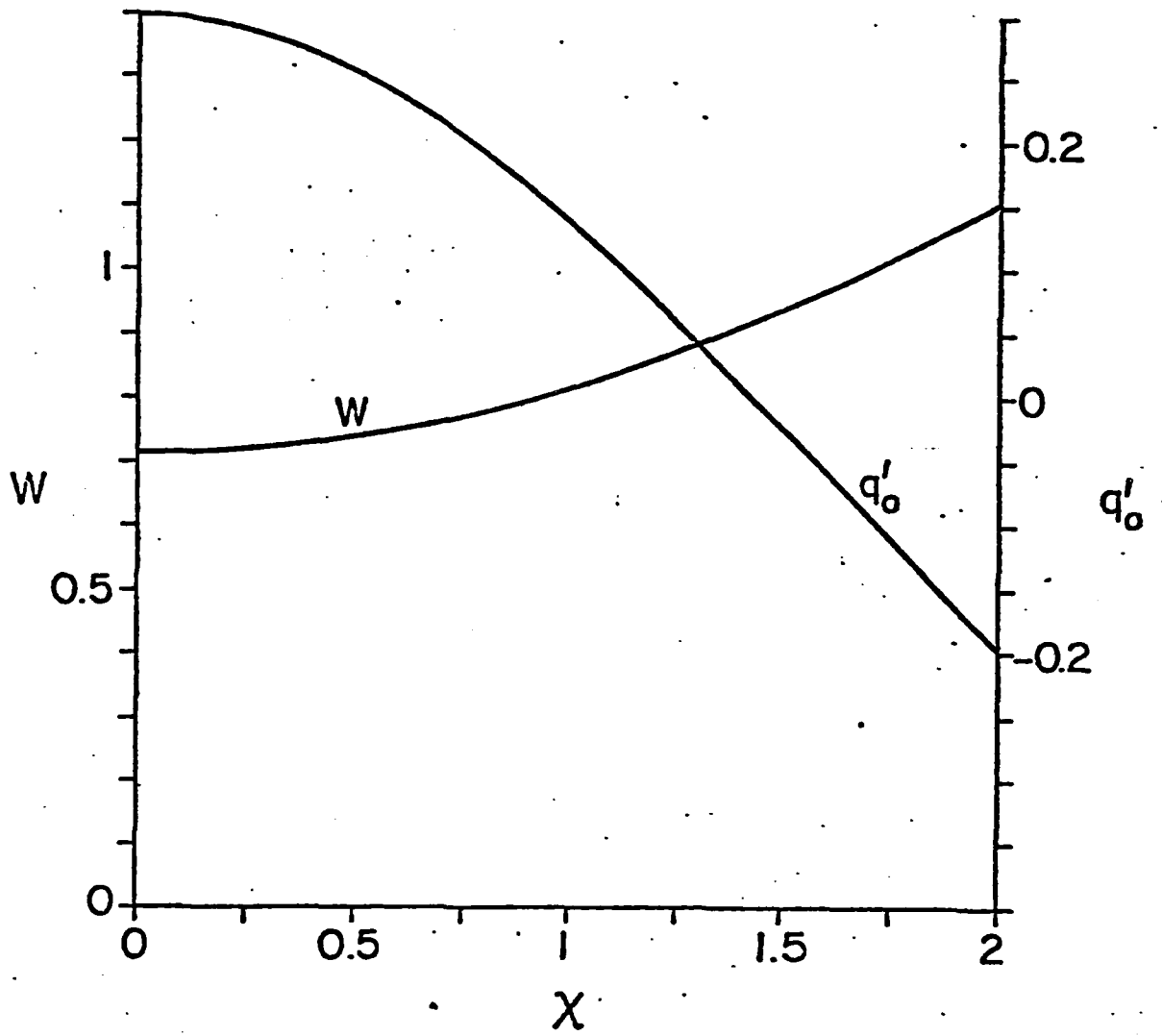


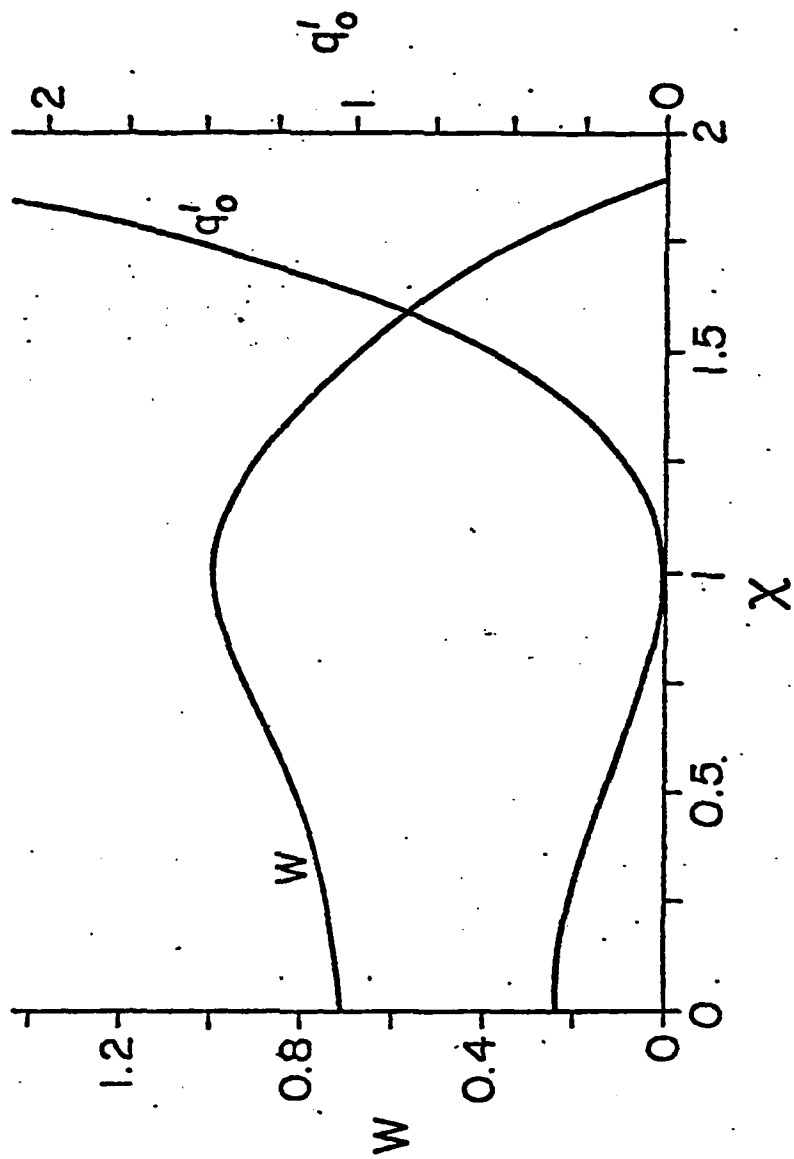












REPORT DOCUMENTATION PAGE		READ INSTRUCTIONS BEFORE COMPLETING FORM
1. REPORT NUMBER 155	2. GOVT ACCESSION NO.	3. RECIPIENT'S CATALOG NUMBER
4. TITLE (and Subtitle) LECTURES ON MATHEMATICAL COMBUSTION Lectuer 10: Free-Boundary Problems		5. TYPE OF REPORT & PERIOD COVERED Interim Technical Report
		6. PERFORMING ORG. REPORT NUMBER
7. AUTHOR(s) J.D. Buckmaster and G.S.S. Ludford		8. CONTRACT OR GRANT NUMBER(s) DAAG29-81-K-0127
9. PERFORMING ORGANIZATION NAME AND ADDRESS Theoretical and Applied Mechanics Cornell University, Ithaca, NY 14853		10. PROGRAM ELEMENT, PROJECT, TASK AREA & WORK UNIT NUMBERS P-18243-M
11. CONTROLLING OFFICE NAME AND ADDRESS U. S. Army Research Office Post Office Box 12211 Research Triangle Park, NC 27709		12. REPORT DATE January 1983
		13. NUMBER OF PAGES 30
14. MONITORING AGENCY NAME & ADDRESS (if different from Controlling Office)		15. SECURITY CLASS. (of this report) unclassified
		15a. DECLASSIFICATION/DOWNGRADING SCHEDULE
16. DISTRIBUTION STATEMENT (of this Report) Approved for public release: distribution unlimited.		
17. DISTRIBUTION STATEMENT (of the abstract entered in Block 20, if different from Report) NA		
18. SUPPLEMENTARY NOTES THE VIEW, OPINIONS, AND/OR FINDINGS CONTAINED IN THIS REPORT ARE THOSE OF THE AUTHOR(S) AND SHOULD NOT BE CONSTRUED AS AN OFFICIAL DEPARTMENT OF THE ARMY POSITION, POLICY, OR DECISION, UNLESS SO DESIGNATED BY OTHER DOCUMENTATION.		
19. KEY WORDS (Continue on reverse side if necessary and identify by block number) Free-boundary problems, δ -function model, hydrodynamic and Burke-Schumann limits, slender flames, Burke-Schumann problem, similarity solution, NEF tips, Stephan problem, negative flame speed, flashback and blow-off, shear and strain stretch, method of lines.		
20. ABSTRACT (Continue on reverse side if necessary and identify by block number) Throughout these lectures we have ensured that the reaction terms vanish everywhere except in a thin (flame) sheet, whose location has to be found as part of the solution. So far this free boundary has been either a plane, a circular cylinder, a sphere, or a perturbation of one of these; we now consider problems with more complicated free boundaries. ↑ -over-		

- (i) Adopt the δ -function model discussed in lecture 7.
- (ii) Take the hydrodynamic limit.
- (iii) Take the Burke-Schumann limit.
- (iv) Use activation-energy asymptotics.

In this lecture, which is an expanded version of Buckmaster (1982), we shall briefly mention examples of (ii) and (iii), but most of the discussion will deal with parabolic problems for premixed flames that arise from (iv).

**DA
FILE**